Powder Technology 204 (2010) 188–193

Contents lists available at ScienceDirect

Powder Technology

journal homepage: www.elsevier.com/locate/powtec

Synthesis and characterization of $La_{0.85}Sr_{0.15}Ga_{0.80}Mg_{0.20}O_{2.825}$ by glycine combustion method and EDTA combustion method

Min Shi *, Miansong Chen, Ruzhong Zuo, Yudong Xu, Hailin Su, Lei Wang, Tao Yu

School of Materials Science and Engineering, Hefei University of Technology, Hefei 230009, PR China

ARTICLE INFO

Article history:
Received 10 February 2010
Received in revised form 8 July 2010
Accepted 19 July 2010
Available online 27 July 2010

Keywords:
Glycine combustion method
EDTA combustion method
Ionic conductivity
Sr and Mg-doped $LaGaO_3$

ABSTRACT

The powders of $La_{0.85}Sr_{0.15}Ga_{0.80}Mg_{0.20}O_{2.825}$(LSGM) were synthesized by glycine combustion method (GCM) and EDTA combustion method (EDTACM). XRD results show that the main phase (LSGM) exists in the uncalcined powders synthesized by GCM. The LSGM materials are composed of the main phase without secondary phases when calcined at 1300 °C. The LSGM materials contain fewer amounts of secondary phases than those prepared by EDTACM at the same calcination temperature. The conductivities of LSGM increase with the increase of testing temperature. The ionic conductivities of LSGM prepared by GCM and EDTACM were calculated to be 0.053 S cm^{-1} and 0.060 S cm^{-1} at 800 °C, respectively. The curve of $\ln(\sigma T)$ vs. $1/T$ exists two straight lines. It indicates that activation energy of oxygen-vacancy motion at lower temperatures is greater than that at higher temperatures.

1. Introduction

Solid oxide fuel cells (SOFCs) have attracted much attention for they offer a pollution-free energy source with great current density and conversion efficiency [1–3]. The key materials for SOFCs are solid electrolytes. Yttria-stabilized zirconia (YSZ) is the most widely used solid electrolyte material in SOFCs[1,3,4]. But ionic conductivity of YSZ decreases quickly with the decrease of the working temperature [5]. Therefore YSZ need be used at higher temperature (800–1000 °C) [4,6]. But this leads to physical and chemical degradation of SOFCs component, interface reaction between electrolytes and electrolytes [1–4]. In order to reduce the operating temperature of SOFC, designing and developing novel intermediate-temperature (IT) electrolytes for IT-SOFC operating temperature over 500–800 °C has now become one of the major responsibilities for SOFC developers [2].

Ishihara et al. [7], Feng and Goodenough [8], developed Sr and Mg-doped lanthanum gallate(LSGM). It has now become an attractive new solid electrolyte used at intermediate temperatures (500–800 °C) [8]. The oxide ionic conductivity of LSGM is almost one order of magnitude larger than that of YSZ at same working temperature [1].The oxide ionic conductivity of LSGM at 800 °C is comparable to that of YSZ at 1000 °C. It possesses negligible electronic conductivity at temperatures lower than 800 °C and a stable performance over a long operating period [4]. Its superior ionic conductivity and chemical properties make it a new generation material as an intermediate-temperature solid electrolyte of SOFCs operated at or below 800 °C [9]. But both phase purity and microstructure of LSGM materials depend on synthetic procedure and processing and, as a matter of fact, the synthesis of LSGM without secondary phases is rather difficult [10]. Djurado et al. [11,12] pointed that, for the presences of impurity phases or secondary phases may decrease the conductivity of LSGM greatly. So LSGM with high purity should be prepared. Sr and Mg-doped lanthanum gallate were mainly synthesized by the solid-state reaction method [13,14]. For this method requires, the multiple repetitions of prolonged grinding and thermal treatment is need, the synthesized powder sizes are large (1–10 μm), calcination temperature of powders are greater than 1500 °C and the powders contain many secondary phases [2,15,16]. So many researchers have turned to wet chemical synthesis methods such as sol–gel [17,18], co-precipitation [14], hydrothermal synthesis [18], the amorphous citrate process [12] and the Pechini method [19,20]. Polini et al. [10,21] showed that calcination temperatures as high as 1500 °C were necessary to prepare pure LSGM without secondary phases. Higher calcination temperatures would lead to overgrowth of powders. The combustion method used as a new synthesis route has been developed by Chlik et al. [22,23]. Due to the exothermic effect of combustion, many organic components or inter-phases are decomposed. Materials with small amount of secondary phases can be obtained and calcination temperatures of powders can be decreased.

In this work, LSGM powders were prepared by two combustion methods, i.e. glycine combustion method (GCM) and EDTA combustion method (EDTACM). By comparing two different combustion processes, we are able to obtain LSGM with higher purity and decrease calcination temperatures of LSGM. The phase structures, the

* Corresponding author. Fax: +86 551 2901362.
E-mail address: mrshimin@hotmail.com (M. Shi).

0032-5910/$ – see front matter © 2010 Elsevier B.V. All rights reserved.
doi:10.1016/j.powtec.2010.07.020

morphologies and the ionic conductivities of LSGM prepared by two combustion methods were also investigated in detail.

2. Experimental

2.1. Powder synthesis and sample preparation

The powders of Sr and Mg-doped lanthanum gallate ($La_{0.85}Sr_{0.15}Ga_{0.8}Mg_{0.2}O_{2.825}$, hereinafter abbreviated as LSGM) were prepared by glycine combustion method (GCM) and EDTA combustion method (EDTACM). La_2O_3 (purity>99.95%), Ga_2O_3 (purity>99.95%), SrO (purity>99.95%), and MgO (purity>99.95%) were used as starting materials. To remove adsorbed H_2O or CO_2, La_2O, Ga_2O_3 and MgO were precalcined at 1000 °C for 6 h; $SrCO_3$ were precalcined at 800 °C for 6 h. According to the stoichiometry of LSGM, stoichiometric amount of Ga_2O_3, La_2O_3, MgO and $SrCO_3$ were first dissolved into HNO_3 to obtain four corresponding nitrate solutions. The above-mentioned solutions were mixed in a glass beaker to get a uniform nitrate solution. For glycine($C_2H_5NO_2$) combustion method, the stoichiometric molar ratio of glycine to oxidant is 1.57:1,considering a little amount of HNO_3 remaining in the nitrate solution, the molar ratio of glycine to oxidant need to be raised to 1.7:1. The glycine was dissolved in the above-mentioned solution. The solution was heated and sufficient water was evaporated. It began to froth and spontaneously burn violently. In this way, the homogeneous white powders were obtained within several minutes. But by the sol–gel method or by solid-state reaction method, it will take several hours or several days. According to propellant chemistry, the combustion gases are generally CO_2, H_2O and N_2, a possible reaction equation of combustion can be written as follows:

$$80La(NO_3)_3 + 20Sr(NO_3)_2 + 85Ga(NO_3)_3 + 15Mg(NO_3)_2 + 313\frac{8}{9}C_2H_5NO_2 \rightarrow 100La_{0.8}Sr_{0.2}Ga_{0.85}Mg_{0.15}O_{2.825} + 627\frac{7}{9}CO_2 + 784\frac{13}{18}H_2O + 439\frac{4}{9}N_2$$

For $C_{10}H_{16}N_2O_8$ (EDTA) combustion method, according to the stoichiometry of LSGM, stoichiometric amount of EDTA, used as a chelating agent, was added into above-mentioned nitrate solution. A calculated amount of citric acid ($C_6H_8O_7$), i.e. 1 mol of trivalent cation needs 1 mol of citric acid and 1 mol of divalent cation needs 2/3 mol of citric acid, was then dissolved. NH_4NO_3 was used as ignition. A certain amount of NH_4NO_3 (the molar ratio of NH_4NO_3 to EDTA is 1:2.) was added. The pH value of nitrate solution was adjusted to 7–8 by adding ammonia to the solution to avoid precipitation. The aqueous solution was heated in a baker, and sufficient water was evaporated until the solution boiled, began to bubble up and burn slowly. The possible reaction equation of combustion is as follows:

$$80La(NO_3)_3 + 20Sr(NO_3)_2 + 85Ga(NO_3)_3 + 15Mg(NO_3)_2 + 70\frac{5}{8}C_{10}H_{16}N_2O_8 \rightarrow 100La_{0.8}Sr_{0.2}Ga_{0.85}Mg_{0.15}O_{2.825} + 706\frac{1}{4}CO_2 + 565H_2O + 353\frac{1}{8}N_2$$

In order to investigate the evolution of phase constitution with calcination temperature, the obtained powders prepared by two combustion method were homogenized in a ceramic mortar and calcined under temperatures ranging from 1200 to 1400 °C. The powders, synthesized by two combustion methods, precalcined at 1000 °C, were pressed uni-axially into $\Phi 12 \times 2$ mm cylindrical samples under 200 MPa for 1 min. The compact samples were then calcined in an air box furnace at 1400 °C for 6 h at a heating rate of 5 °C min^{-1}.

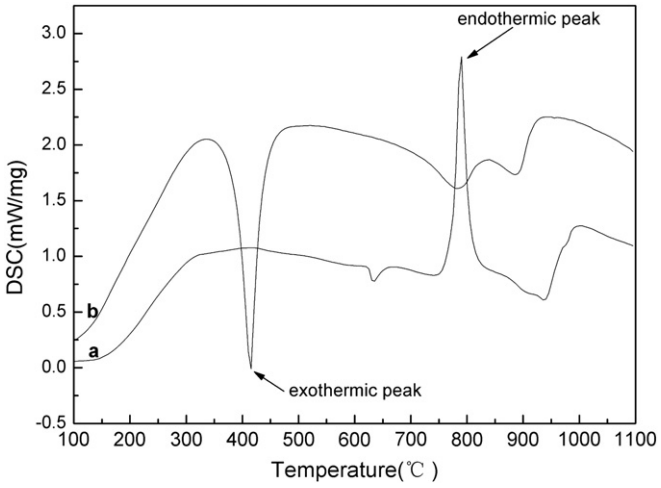

Fig. 1. DSC curves of uncalcined powders synthesized by different methods; (a) synthesized by GCM; (b) by EDTACM.

2.2. Characterization

The thermal effect of the powders synthesized by GCM and EDTACM were investigated by DSC, Differential Scanning Calorimetry (NETZSCH, STA409C) at rate of 5 °C min^{-1} in air. The phase analysis of the uncalcined and calcined powders prepared by two combustion methods were performed, using a powder X-ray diffractometer (Rigaku,D/Max-rB) with CuKα at a scanning speed of 2° min^{-1}.The XRD patterns were analyzed with MDI Jade 5.0 software to calculate Lattice parameters and cell volume of the powders. The compositions of calcined powders prepared by two combustion methods were analyzed by Inductively Coupled Plasma Mass Spectrometer (Thermo fisher Scientific, X Series 2). The particle size and morphology of the LSGM powders prepared by two combustion methods were examined by transmission electron microscope (Hitachi, H800). Microstructures of the samples were observed by scanning electron microscope (Cambridge, S-360). The ionic conductivities of LSGM samples at different testing temperature, prepared by two combustion methods, calcined at 1400 °C, were calculated by the AC impendence spectra method, using an electrochemical workstation (Chenhua, CHI604A), analyzed with the Zsimp Win analysis software.

3. Results and discussion

3.1. DSC analysis

The DSC curves of uncalcined LSGM powders prepared by the GCM and EDTACM were shown in Fig. 1, respectively. For GCM, it can be seen that there exist a weak exothermic peak at about 630 °C which may be due to the complex decomposition reactions of organics [3], an strong endothermic peak at about 800 °C which may be attributed to decomposition of the crystal process of the secondary phases, an obvious endothermic peak at about 1000 °C which corresponds to the transformation of secondary phases to the main phase [24]. For EDTACM, it can also be seen that there exist a distinct endothermic peak at about 330 °C and an obvious exothermic peak at about 410 °C, which may be attributed to the decomposition and combustion of the organics, such as EDTA and citric acid. At a temperature range of 600–800 °C, there exist two exothermic peaks and an endothermic peak, which may be related to the decomposition of carbonate and nitrate. At about 1000 °C, there exists an endothermic peak, which corresponds to the transformation of secondary phases to the main phase [15]. This is in agreement with the DSC result of LSGM powders prepared by the GCM.

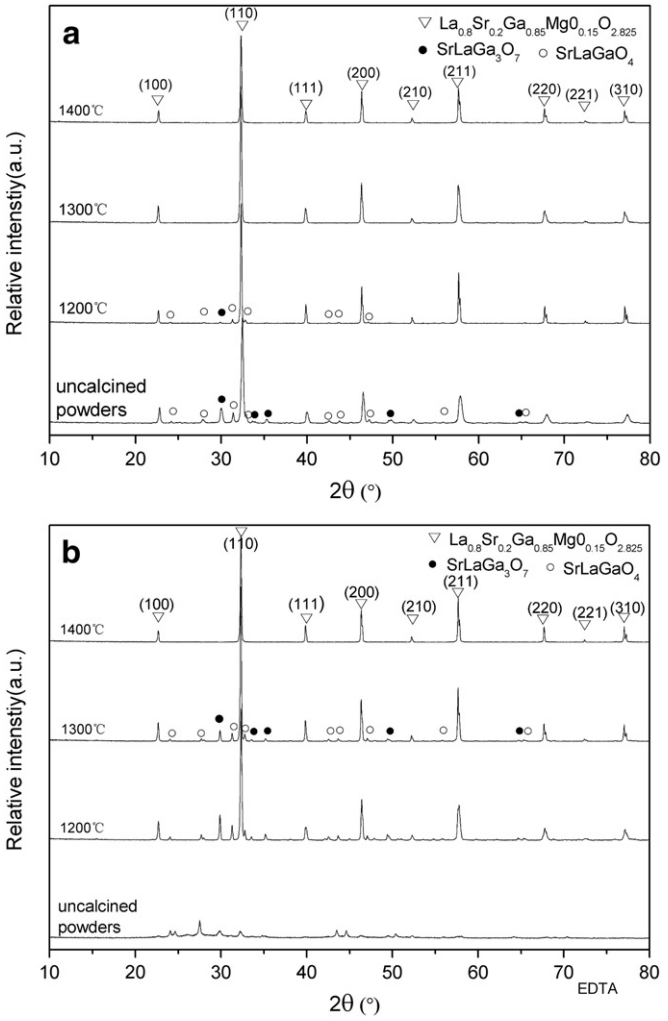

Fig. 2. XRD patterns of powders and samples calcined at different temperatures for 6 h; (a) synthesized by GCM; (b) synthesized by EDTACM.

3.2. Phase analysis of XRD

Fig. 2(a) and (b) shows X-ray diffraction spectra (XRD) of LSGM powders prepared by GCM and EDTACM, respectively. From Fig. 2(a), it can be seen that, in the uncalcined powders, there exist the main phase-$La_{0.8}Sr_{0.2}Ga_{0.85}Mg_{0.15}O_{2.825}$ (JCPDS card No. 52-0022) and a great amount of impurity phases or secondary phases, i.e. $SrLaGa_3O_7$ (JCPDS card No.45-0637) and $SrLaGaO_4$ (JCPDS card No. 24-1208). But for other powder synthesis methods, it is very difficult to obtain the main phase (LSGM) in the uncalcined powders [18]. Fig. 2(a) also illustrates powders calcined at 1200 °C still contain a certain amount of secondary phases except the main phase. Polini et al. [10,17,26] have estimated the relative amounts of secondary phases approximately by calculating As/Ap, the ratio of the total integrated intensities of the most intense XRD peaks of these secondary phases over the integrated intensity of the most intense peak of LSGM. From Fig. 2(a), the relative amount of $SrLaGa_3O_7$ and $SrLaGaO_4$ was estimated by calculating As/Ap, the ratio of the total integrated intensities of the most intense XRD peaks of these secondary phases over the integrated intensity of the (110) peak of LSGM. It is about 4%. The relative amount of secondary phases decreased with the increase of sintering temperature. With the further increase of temperature, the fractions of secondary phases decreased remarkably. This shows that the secondary phases has transformed partly to the main phase. Nearly no secondary phases can be detected when calcination temperature reaches 1300 °C. The compositions of LSGM powders calcined at 1300 °C were analyzed by Inductively Coupled Plasma Mass Spectrometer (ICP-MS).The procedures for ICP-MS are as follows, a certain amount of LSGM powders was firstly weighed, dissolved in aqua regia to obtain a solution, then the solution was dissolved in another standard solution to obtain a new solution, the new solution was analyzed by ICP-MS, finally mass of La, Sr, Ga, Mg can be obtained. Mass of LSGM powders minus total mass of La, Sr, Ga and Mg in LSGM powders gives mass of O in LSGM powders. Therefore the molar ratio of La, Sr, Ga, Mg, and O in LSGM powders can be deduced. ICP-MS analyses indicated that the average molar ratio of La, Sr, Ga, Mg, and O for powders calcined at 1300 °C is 0.849:0.151:0.799:0.201:2.827. This is close to the stoichiometric ratio of $La_{0.85}Sr_{0.15}Ga_{0.8}Mg_{0.2}O_{2.825}$. However, Khanlou et al. [22,27,28] indicated that there was no main phase existing in the uncalcined powders; even after calcination at 1400 °C for 6 h, the powders were still not composed of a single phase and contained about 5 vol% of the secondary phases. LSGM powders with high purity can be obtained by using the GCM when calcined at 1300 °C. Thus the calcination temperature of LSGM powders prepared by GCM is at least 100 °C lower than those prepared by solid-state reaction or other wet chemical synthesis methods, as reported in literature [2,11,15,22]. This helps to avoid the formation of non-stoichiometric powders [22].

Fig. 2(b) indicates that there is nearly no main phase in the uncalcined powders prepared by EDTACM, the powders calcined at 1300 °C still contain a certain amount of secondary phases, the relative amounts of $SrLaGa_3O_7$ and $SrLaGaO_4$, estimated by calculating As/Ap, is about 12%. Fig. 2(b) also shows that nearly no secondary phases can be detected when calcination temperature reaches 1400 °C. ICP-MS analyses indicated that the average molar ratio of La, Sr, Ga, Mg, and O for powders calcined at 1400 °C is 0.851:0.148:0.802:0.202:2.824. This is also close to the stoichiometric ratio of $La_{0.85}Sr_{0.15}Ga_{0.8}Mg_{0.2}O_{2.825}$. Compared Fig. 2(a) with Fig. 2(b), it can be seen that synthesized powders prepared by GCM contain fewer secondary phases than those prepared by EDTACM at the same calcination temperature. The reason is that by GCM, the combustion process is more violent and it produces more heat and higher temperature, makes phase transformation more completely. Therefore LSGM materials contain fewer amounts of secondary phases than those prepared by EDTACM at the same calcination temperature. The calcination temperatures of powders synthesized by GCM are 100 °C lower than those synthesized by EDTACM. It can be inferred that GCM is a better way to obtain LSGM materials with high purity. Owing to the decrease of secondary phases which lower the conductivity of LSGM, it will help to acquire LSGM electrolyte materials with higher ionic conductivities [5].

The XRD results, analyzed with MDI Jade 5.0 software, were shown in Table 1. It can be seen that, the lattice parameters and cell volume of LSGM, prepared by GCM and EDTACM, are a little greater than those of undoped lanthanum gallate ($LaGaO_3$, JCPDS card no: 89-4796). For ionic radius of doped Sr is greater than that of La, ionic radius of doped Mg is greater than that of Ga. This leads to lattice expansion of $LaGaO_3$ crystal when La and Ga are partly replaced by Sr and Mg, respectively. Table 1 also indicates that a small amount of dissolution of Sr and Mg to $LaGaO_3$ does not make crystal structure of $LaGaO_3$ changed.

Table 1
Crystal structure, Lattice parameters, Cell volume of LSGM, synthesized by GCM and EDTACM, calcined at 1400 °C for 6 h.

Materials	Crystal structure	Lattice parameters (Å)	Cell volume (Å^3)
LSGM(GCM)	Cubic	a = b = c = 3.913	59.92
LSGM(EDTACM)	Cubic	a = b = c = 3.912	59.86
$LaGaO_3$	Cubic	a = b = c = 3.886	58.68

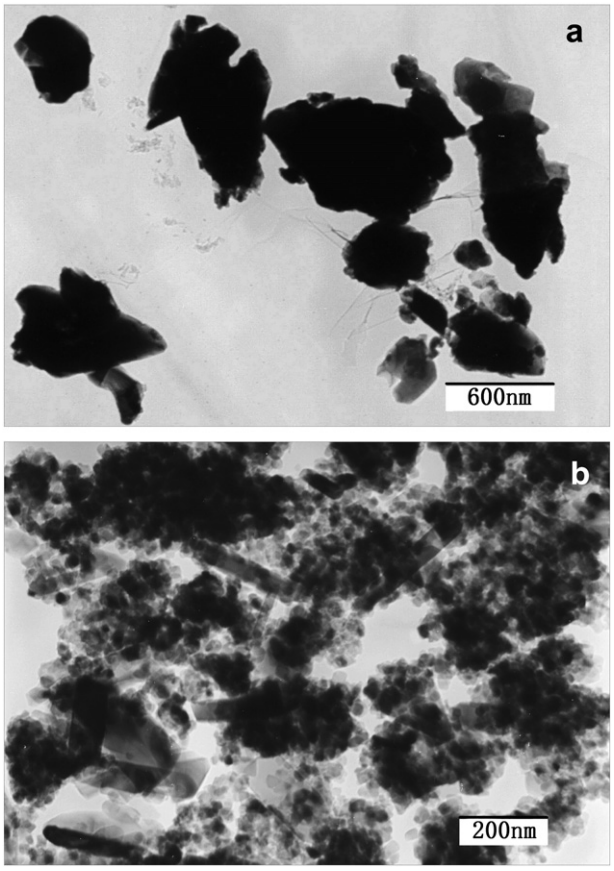

Fig. 3. TEM micrographs of powders; (a)synthesized by GCM, calcined at 1400 °C for 6 h; (b)synthesized by EDTACM, calcined at 1400 °C for 6 h.

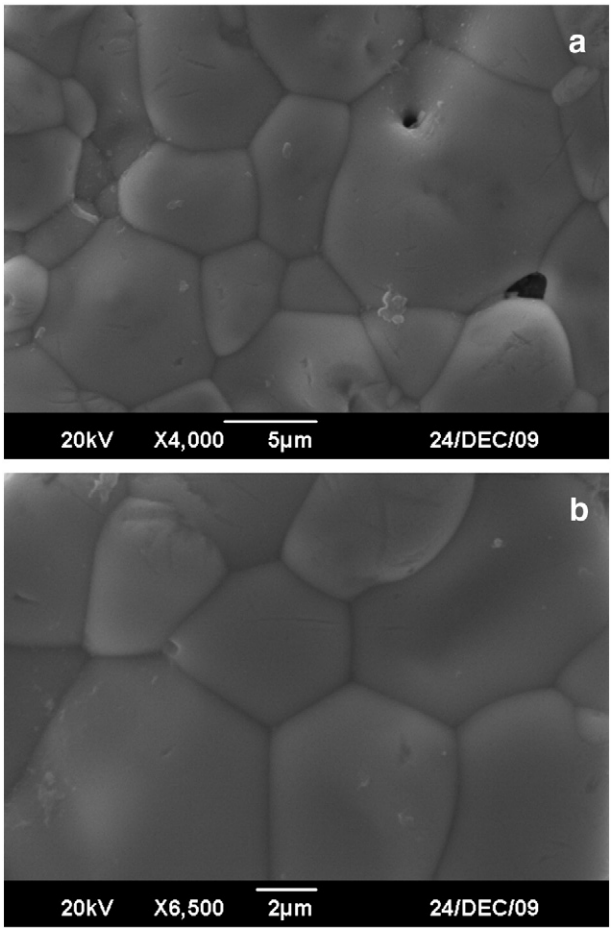

Fig. 4. SEM micrographs of LSGM samples; (a) synthesized by GCM, calcined at 1400 °C for 6 h; (b) synthesized by EDTACM, calcined at 1400 °C for 6 h.

3.3. Morphology and microstructure

Fig. 3(a) and (b) show TEM micrographs of powders, synthesized by GCM and EDTACM, respectively. Fig. 3(a) shows that the powders form agglomerates, sizes of the powders range from about 200 nm to about 900 nm, the distributions of sizes of the powders are wide and the average size of powders is about 600 nm. Fig. 3(b) also shows that the powders form agglomerates, sizes of the powders range from about 70 nm to about 110 nm, the distributions of sizes of the powders are narrow and the average size of powder is about 90 nm. Compared Fig. 3(a) with Fig. 3(b), it can be seen that the powders with smaller powder sizes can be obtained by EDTACM.

Fig. 4(a) and (b) show the SEM micrographs of LSGM samples, prepared by GCM and EDTACM, respectively. Fig. 4(a) indicated that the average crystallite size of LSGM materials were about 5 μm, only a small number of small pores or pin holes can be seen on the surface of sample, which will decrease the ionic conductivity of LSGM. From Fig. 4(b), it can be seen that no cracks, pores or pin holes were seen on the surface of LSGM sample prepared by EDTACM and the average crystallite size of LSGM materials were about 6 μm.

3.4. Conductivity of LSGM samples

$LaGaO_3$ (ABO_3) possesses perovskite structure. For $La_{1-x}Sr_xGa_{1-y}Mg_yO_3$, La in position A of perovskite structure is partially replaced by Sr and Ga in position B is partially replaced by Mg. On the basis of electric neutrality principle, oxygen vacancies form. Oxygen motion from one vacancy to adjacent vacancy gives rise to conductivity.

The AC impedance spectra of LSGM samples prepared by GCM and EDTACM at different temperatures are given in Fig. 5(a) and (b), respectively. It indicates that there exists an arc, which corresponds to interface resistance between electrolyte and electrodes. With the increase of testing temperatures, the arcs move towards left and are depressed to a semicircle. The conductivities can be calculated from Eq. (1)

$$\sigma = L / RA \tag{1}$$

where σ is ionic conductivity, L and A are the thickness and area of the pellets, R is electrolyte resistance, which can be obtained from the impedance spectra [16]. The calculated conductivities of LSGM samples prepared by two combustion methods are shown in Fig. 6. It can be seen that, the ionic conductivities of LSGM, prepared by two combustion methods, increase with the increase of testing temperature. This is due to the acceleration of oxygen-vacancy motion with the increase of testing temperature. At same testing temperature, the conductivities of LSGM samples prepared by EDTACM are greater than that of LSGM samples prepared by GCM. It may be due to unfavorable effect of a small number of small pores in LSGM prepared by GCM (as shown in Fig. 4(a)) on ionic conductivities. The pores trapped in grain and grain boundaries block oxygen ion migration, decrease the ionic conductivity consequently. At 800 °C, the ionic conductivities of LSGM samples prepared by GCM and EDTACM are 0.053 S cm^{-1} and 0.060 S cm^{-1}, respectively, which is obviously greater than those reported in literatures [2,25], as shown in Table 2.

From Arrhenius equation, Eq. (2) or (3) can be derived as follows [14]:

$$\sigma T = B \exp(-E / kT) \tag{2}$$

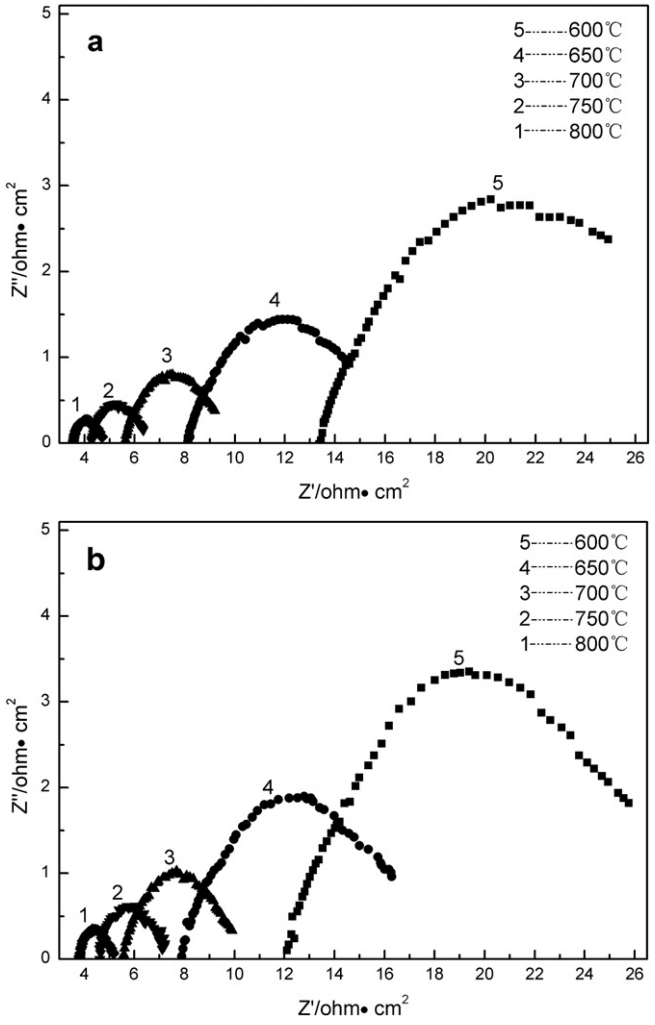

Fig. 5. AC impedance spectra of LSGM samples, at different testing temperatures; (a) synthesized by GCM, calcined at 1400 °C for 6 h; (b) synthesized by EDTACM, calcined at 1400 °C for 6 h.

or

$$\ln(\sigma T) = \ln B - E/kT \quad (3)$$

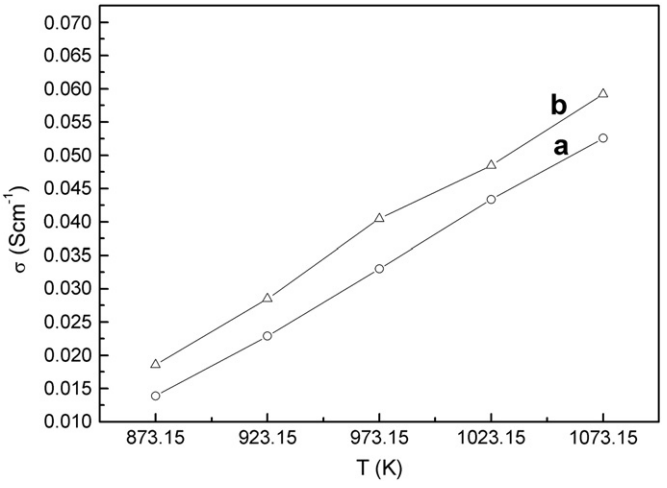

Fig. 6. Conductivities of LSGM samples, at different temperatures; (a) synthesized by GCM, calcined at 1400 °C for 6 h; (b) synthesized by EDTACM calcined at 1400 °C for 6 h.

Table 2
The ionic conductivity of LSGM for this work and other researchers' work [2,25].

Materials	Calcined temperature(℃)	Testing temperature(℃)	σ (S cm^{-1})
LSGM prepared by GCM	1400	800	0.053
LSGM prepared by EDTACM	1400	800	0.060
LSGM reported in literature[2]	1400	800	0.0179
LSGM reported in literature[25]	1400	800	0.0385

where σ stands for ionic conductivity, B stands for ratio factor, k stands for Boltzmann constant, T stands for testing temperature, and E stands for activation energy of oxygen-vacancy motion, i.e. energy for oxygen motion from one vacancy to adjacent vacancy.

From Eq. (3), It can be seen that there should exist linear relationship between $\ln(\sigma T)$ and $1/T$. Fig. 7 shows variation of $\ln(\sigma T)$ with $1/T$. It can be seen that there exists two straight lines intersecting at T^* (T^* is about 700 °C), though it is not very obvious and appears as a gradual changeover. According to the literature [12,14], such a changeover could be used to explain the change of activation energy. From Fig. 7, E was deduced. For LSGM prepared by GCM, $E_1 = 0.709$ eV (E_1, activation energy at $T<T^*$), $E_2 = 0.515$ eV (E_2, activation energy at $T>T^*$). This shows that the activation energy of oxygen-vacancy motion at lower temperatures ($T<T^*$) is greater than that at higher temperatures ($T>T^*$). The reason is that the oxygen vacancies are progressively trapped out into the clusters with decreasing temperature below T^*, while they are dissolved into the matrix of oxygen sites from the clusters and the activation energy becomes small with increasing temperature above T^* [17]. For LSGM prepared by EDTACM, Fig. 7 shows the similar result. From Fig. 7, activation energies E of LSGM prepared by EDTACM were also deduced, i.e. $E_1 = 0.644$ eV, $E_2 = 0.424$ eV. The values of activation energies were found to be smaller than that reported in the relevant literature ($E_1 = 1.073$ eV, $E_2 = 0.845$ eV) [12]. From Eq. (3), it can be seen that the ionic conductivity will increase with the decrease of activation energy.

4. Conclusions

LSGM powders were synthesized by GCM and EDTACM. The XRD pattern shows that the main phase (LSGM) exists in the uncalcined powders prepared by GCM. With the increase of temperature, the

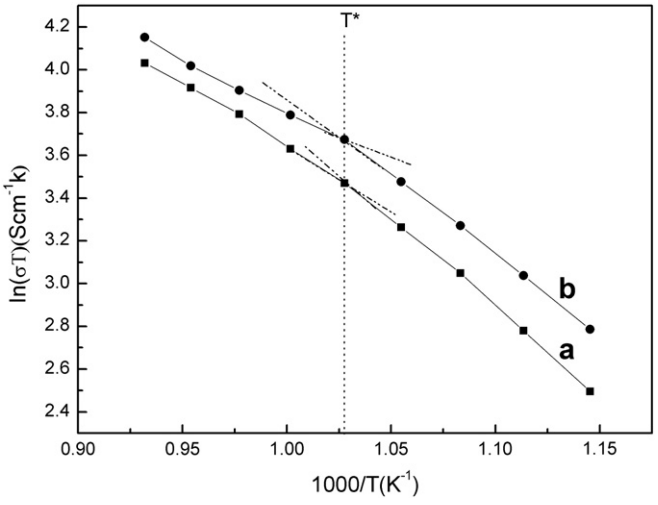

Fig. 7. Arrhenius plot of ionic conductivity of the LSGM samples; (a) synthesized by GCM, sintered at 1400 °C for 6 h; (b) synthesized by EDTACM, sintered at 1400 °C for 6 h.

fractions of secondary phases decreased remarkably. LSGM materials are composed of the main phase without secondary phases when calcined at 1300 °C. But no main phase (LSGM) exists in the uncalcined powders prepared by EDTACM. LSGM materials are composed of the main phase without secondary phases when calcined at 1400 °C. The GCM is a better way to obtain LSGM materials with high purity. The calcination temperature of LSGM powders prepared by GCM is 100 °C lower than those prepared by EDTACM. The average grain sizes of powders synthesized by EDTACM are smaller than those synthesized by GCM. The ionic conductivities of LSGM, prepared by two combustion methods, increase with the increase of testing temperature. At same testing temperature, the conductivities of LSGM prepared by EDTACM are greater than that of LSGM prepared by GCM. The curve of $\ln(\sigma T)$ vs $1/T$ exists two straight lines intersecting at T^* (T^* is about 700 °C). This shows that activation energy of oxygen-vacancy motion at lower temperatures is greater than that at higher temperatures.

Acknowledgments

The authors wish to acknowledge the financial support of this research from Specialized Research Fund for the Doctoral Program of Higher Education of China and the Scientific Research Fund of Hefei University of Technology for Doctors Degree.

References

[1] F. Bozza, R. Polini, E. Traversa, High performance anode-supported intermediate temperature solid oxide fuel cells (IT-SOFCs) with $La_{0.8}Sr_{0.2}Ga_{0.8}Mg_{0.2}O_{3-\delta}$ electrolyte films prepared by electrophoretic deposition, Electrochem. Commun. 11 (2009) 1680–1683.
[2] L.G. Cong, T.M. He, Y.A. Ji, P.F. Guan, Y.L. Huang, W.H. Su, Synthesis and characterization of IT-electrolyte with perovskite structure $La_{0.8}Sr_{0.2}Ga_{0.85}Mg_{0.15}O_{3-\delta}$ by glycine–nitrate combustion method, J. Alloys Compd. 348 (2003) 325–331.
[3] B. Liu, L.D. Tang, Y. Zhang, Preparation and characterization of $La_{0.9}Sr_{0.1}Ga_{0.8}Mg_{0.2}O_{3-\delta}$ thin film on the porous cathode for SOFC, Int. J. Hydrogen Energy 34 (2009) 440–445.
[4] T.Y. Chen, K.Z. Fung, Comparison of dissolution behavior and ionic conduction between Sr and/or Mg doped $LaGaO_3$ and $LaA1O_3$, J. Power Sources 132 (2004) 1–10.
[5] M. Shi, Y.D. Xu, A.P. Liu, N. Liu, C. Wang, P. Majewski, F. Aldinger, Synthesis and characterization of Sr- and Mg-doped Lanthanum gallate electrolyte materials prepared via the Pechini method, Mater. Chem. Phys. 114 (2009) 43–46.
[6] I.N. Sora, R. Pelosato, A. Simone, L. Montanaro, F. Maglia, G. Chiodelli, Characterization of LSGM films obtained by electrophoretic deposition (EPD), Solid State Ionics 177 (2006) 1985–1989.
[7] T. Ishihara, H. Matsuda, Y. Takita, Doped $LaGaO_3$ perovskite type oxide as a new oxide ionic conductors, J. Am. Chem. Soc. 116 (1994) 3801–3804.
[8] M. Feng, J.B. Goodenough, A superior oxide-ion electrolyte, Eur. J. Solid State Inorg. Chem. 31 (1994) 663–672.
[9] S. Pathak, D. Steinmetz, J. Kuebler, E.A. Payzant, N. Orlovskaya, Mechanical behavior of $La_{0.8}Sr_{0.2}Ga_{0.8}Mg_{0.2}O_3$ perovskites, Ceram. Int. 35 (2009) 1235–1241.
[10] R. Polini, A. Falsetti, E. Traversa, Sol–gel synthesis and characterization of Co-doped LSGM perovskites, J. Eur. Ceram. Soc. 25 (2005) 2593–2597.
[11] E. Djurado, M. Labeau, Second phases in doped lanthanum gallate perovskites, J. Eur. Ceram. Soc. 18 (1998) 1397–1404.
[12] R. Polini, A. Pamio, E. Traversa, Effect of synthetic route on sintering behaviour, phase purity and conductivity of Sr- and Mg-doped $LaGaO_3$ perovskites, J. Eur. Ceram. Soc. 24 (2004) 1365–1370.
[13] P.S. Cho, S.Y. Park, Y.H. Cho, S.J. Kim, Y.C. Kang, T. Mori, J.H. Lee, Preparation of LSGM powders for low temperature sintering, Solid State Ionics 180 (2009) 788–791.
[14] K. Huang, M. Feng, J.B. Goodenough, Sol–gel synthesis of a new oxide-ion conductor Sr- and Mg-doped $LaGaO_3$ perovskite, J. Am. Ceram. Soc. 79 (1996) 1100–1104.
[15] T.Y. Chen, K.Z. Fung, Synthesis of and densification of oxygen-conducting $La_{0.8}Sr_{0.2}Ga_{0.8}Mg_{0.2}O_{2.8}$ nano powder prepared from a low temperature hydrothermal urea precipitation process, J. Eur. Ceram. Soc. 28 (2008) 803–810.
[16] F. Maglia, U. Anselmi-Tamburini, G. Chiodelli, H.E. Camurlu, M. Dapiaggi, Z.A. Munir, Electrical, structural, and microstructural characterization of nanometric $La_{0.9}Sr_{0.1}Ga_{0.8}Mg_{0.2}O_{3-\delta}$(LSGM) prepared by high-pressure spark plasma sintering, Solid State Ionics 180 (2009) 36–40.
[17] Y.L. Zhai, C. Ye, F. Xia, J.Z. Xiao, L. Dai, Y.F. Yang, Y.Q. Wang, Preparation of $La_{0.8}Sr_{0.2}Ga_{0.83}Mg_{0.17}O_{2.815}$ powders by microwave-induced poly(vinyl alcohol) solution polymerization, J. Power Sources 162 (2006) 146–150.
[18] K. Huang, J.B. Goodenough, Wet chemical synthesis of Sr- and Mg-doped $LaGaO_3$, a perovskite-type oxide-ion conductor, J. Solid State Chem. 136 (1998) 274–283.
[19] A.C. Tas, P.J. Majewski, F. Aldinger, Chemical preparation of pure and strontium- and/or magnesium-doped lanthanum gallate powders, J. Am. Chem. Soc. 83 (2000) 2954–2960.
[20] A. Tarancon, G. Dezanneau, J. Arbiol, Synthesis of nanocrystalline materials for SOFC applications by acrylamide polymerisation, J. Power Sources 118 (2003) 256–264.
[21] P. Majewski, M. Rozumek, C.A. Tas, F. Aldinger, Processing of (La, Sr)(Ga, Mg)O3 solid electrolyte, J. Electroceram. 8 (2002) 65–73.
[22] A. Ahmad-Khanlou, F. Tietz, D. Stver, Material properties of $La_{0.8}Sr_{0.2}Ga_{0.9+x}Mg_{0.1}O_{3-\delta}$ as a function of Ga content, Solid State Ionics 135 (2000) 543–547.
[23] L.A. Chick, L.R. Pederson, G.D. Maupin, J.L. Bates, L.E. Thomas, Glycine–nitrate combustion synthesis of oxide ceramic powders, Mater. Lett. 10 (1990) 6–12.
[24] B. Liu, Y. Zhang, $La_{0.9}Sr_{0.1}Ga_{0.8}Mg_{0.2}O_{3-\delta}$ sintered by spark plasma sintering (SPS) for intermediate temperature SOFC electrolyte, J. Alloys Compd. 458 (2008) 383–389.
[25] G.Y. Xu, M. Cao, B. Liu, Comparison of LSGM and LSGMC(8.5) synthesized by advanced pechini method, J. Inorg. Mater. 21 (2006) 612–618.
[26] Y.L. Zhai, C. Ye, J.Z. Xiao, L. Dai, $La_{0.9}Sr_{0.1}Ga_{0.8}Mg_{0.2}O_{3-\delta}$ sintered by spark plasma sintering (SPS) for intermediate temperature SOFC electrolyte, J. Power Sources 163 (2006) 316–322.
[27] K. Huang, R. Tichy, J.B. Goodenough, Superior perovskite oxide-ion conductor; strontium-and magnesium-doped $LaGaO_3$: I, phase relationships and electrical properties, J. Am. Ceram. Soc. 81 (1998) 2565–2575.
[28] J.W. Stevenson, T.R. Armstrong, D.E. McCready, L.R. Pederson, W.J. Weber, Processing and electrical properties of alkaline earth-doped lanthanum gallate, J. Electrochem. Soc. 144 (1997) 3613–3620.